Crystal Structure of Unmodified $tRNA^{Gln}$ Complexed with Glutaminyl-tRNA Synthetase and ATP Suggests a Possible Role for Pseudo-Uridines in Stabilization of RNA Structure†

John G. Arnez‡ and Thomas A. Steitz*

Department of Molecular Biophysics and Biochemistry and Howard Hughes Medical Institute, Yale University, New Haven, Connecticut 06511

Received December 29, 1993; Revised Manuscript Received April 22, 1994®

ABSTRACT: $tRNA_2^{Gln}$ made *in vitro* by transcription with T7 RNA polymerase does not contain the pseudo-uridines at positions 38, 39, and 55, the 4-thiouridine at position 8, or any of the methylated bases found in the $tRNA_2^{Gln}$ made *in vivo*. Cocrystals of unmodified $tRNA_2^{Gln}$ complexed with glutaminyl-tRNA synthetase from *Escherichia coli* are isomorphous with those of the complex with modified $tRNA_2^{Gln}$. A difference electron density map between the complexes with modified and unmodified tRNAs calculated at 2.5-Å resolution shows no differences in the protein or tRNA structures, except for some very small shifts in atoms contacting the thiol at the 4 position of uridine 8 that are required to accommodate the smaller oxygen in the unmodified tRNA. Perhaps the most functionally significant change in the unmodified tRNA is the absence of the specifically bound water molecules that are observed to cross-link the N5 of the pseudo-uridines to their 5′ phosphate. This suggests a possible role for pseudouridinylation in stabilization of the tRNA through water-mediated linking of these modified bases to the backbone, which is consistent with the lower thermal stability of the unmodified tRNA. An identical water-bridging structure is possible at four of the five other psuedo-uridines in known tRNA structures.

Transfer RNAs (tRNAs)[1] from all organisms possess modified nucleotides; these may influence the specificity with which tRNAs bind to various proteins and ribonucleoprotein ribosome (Björk *et al.*, 1987). $tRNA_2^{Gln}$ [2] is methylated at four positions (2′mG18, 2′mG32, 2mA37, and T(=5mU)-54); it has a dihydrouridine at position 20, a 4-thiouridine at position 8, and three pseudo-uridines (Ψ38, Ψ39, and Ψ55) (Yaniv & Folk, 1975). Proton NMR studies of unmodified yeast $tRNA^{Phe}$ have shown that it folds normally and has a structure that resembles its fully modified counterpart (Hall *et al.*, 1989). Similarly, comparisons of ^{19}F NMR spectra of 5-fluorouracil-substituted $tRNA^{Val}$ (5FU-$tRNA^{Val}$) isolated from 5-fluorouracil-treated *Escherichia coli* with those of 5FU-$tRNA^{Val}$ produced by transcription *in vitro* with T7 RNA polymerase have suggested that both the *in vitro* transcript and tRNA produced *in vivo* have similar secondary and tertiary structures when the spectra are measured in the presence of magnesium; they differ markedly, however, in the absence of magnesium (Chu & Horowitz, 1989). Thermal melting profile (Sampson & Uhlenbeck, 1988; Perret *et al.*, 1990b; Derrick & Horowitz, 1993), chemical (Perret *et al.*, 1990b; Chow *et al.*, 1992), and enzymatic probing (Derrick & Horowitz, 1993) studies of native tRNAs and their unmodified counterparts in solution and Mg^{2+}-induced cleavage analyses of $tRNA^{Gln}$, modified and unmodified, bound to glutaminyl-tRNA synthetase (GlnRS) (Beresten *et al.*, 1992) show that nucleotide modifications enhance structural stability of the tRNA molecule. The effect of nucleotide modifications on aminoacylation of tRNAs ranges from none at all, as in $tRNA^{Val}$ (Chu & Horowitz, 1989), through slight enhancement of efficiency, as in $tRNA^{Gln}$ (Jahn *et al.*, 1991), to a substantial definition of the identity of the tRNA, exemplified by $tRNA^{Asp}$ (Perret *et al.*, 1990a). We address here how the lack of post-transcriptional modification affects the structure of $tRNA^{Gln}$ complexed with glutaminyl-tRNA synthetase (GlnRS), by comparing the crystal structures of modified (Rould *et al.*, 1989; Rould *et al.*, 1991) and unmodified $tRNA_2^{Gln}$, complexed with GlnRS and ATP.

Unmodified RNA with authentic 5′ and 3′ termini can be efficiently produced by transcription *in vitro* with phage T7 RNA polymerase (Milligan *et al.*, 1987; Vioque *et al.*, 1988). T7 RNA polymerase requires that a G be the first nucleotide in the transcript (Milligan *et al.*, 1987), whereas native $tRNA_2^{Gln}$ has a U at this position. In the crystal structure of $tRNA_2^{Gln}$ complexed with GlnRS and ATP, the base pair U1-A72 is disrupted by the protein; furthermore, U1 is disordered and is not involved in any RNA–protein interactions (Rould *et al.*, 1989), which suggests that a base substitution at this position would have no effect on the structure of the tRNA or its aminoacylation rate. In this study, two modifications of wild-type $tRNA_2^{Gln}$ [1] (Figure 1) were made *in vitro* and cocrystallized with GlnRS; both had a G at position 1 instead of the original U. One version was otherwise unchanged, which resulted in a G·A mismatch at position 1–72 ($tRNA_{G1}^{Gln}$), while the other had a complementary C at position 72 ($tRNA_{G1\text{-}C72}^{Gln}$) (A. B. DiRenzo and O. C. Uhlenbeck, personal communication). $tRNA_{G1}^{Gln}$ had a relative

† This research was supported by a grant from the NIH.

* Author to whom correspondence should be addressed.

‡ Present address: Institut de Biologie Moléculaire et Cellulaire du CNRS, Laboratoire de Biologie Structurale, 15 rue René Descartes, 67084 Strasbourg Cedex, France.

® Abstract published in *Advance ACS Abstracts,* June 1, 1994.

[1] Abbreviations: RNA, ribonucleic acid; tRNA, transfer RNA; GlnRS, glutaminyl-tRNA synthetase; NMR, nuclear magnetic resonance; ATP, adenosine triphosphate; GTP, guanosine triphosphate; CTP, cytidine triphosphate; UTP, uridine triphosphate; DTT, dithiothreitol; PEG, polyethylene glycol; DNAse, deoxyribonuclease; RNase, ribonuclease; EDTA, ethylenediaminetetraacetic acid.

[2] In this article, $tRNA_2^{Gln}$ stands for native $tRNA^{Gln}$ purified from overexpressing *E. coli*, while $tRNA_{G1}^{Gln}$ and $tRNA_{G1\text{-}C72}^{Gln}$ were produced by transcription *in vitro* with T7 RNA polymerase.

0006-2960/94/0433-7560$04.50/0 © 1994 American Chemical Society

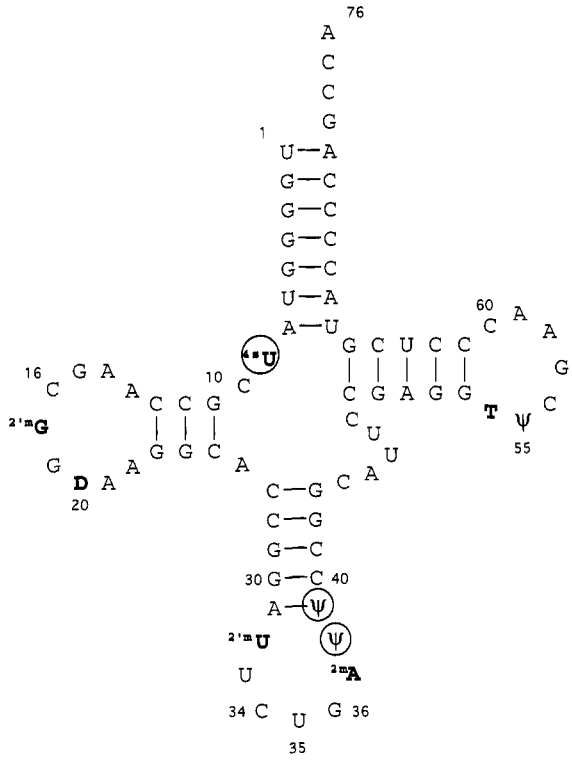

FIGURE 1: Cloverleaf representation of $tRNA_2^{Gln}$. Modified nucleotides are shown in boldface. Circles indicate the modifications observed in this study.

k_{cat}/K_M of 25% compared to $tRNA_2^{Gln}$ that had been purified from *E. coli*, while the k_{cat}/K_M of $tRNA_{G1\text{-}C72}^{Gln}$ was a tenth of that exhibited by $tRNA_{G1}^{Gln}$ (Jahn *et al.*, 1991). The tRNA with the G1·A72 mismatch, complexed with GlnRS, also gave better crystals than its G1-C72 counterpart, allowing the determination of the crystal structure of an unmodified tRNA.

MATERIALS AND METHODS

Production and Purification of Wild-Type GlnRS. GlnRS was purified from heat-induced cells of the *E. coli* strain K12ΔH1Δtrp transformed with overproducing plasmid pMN20 (M. Nichols and D. G. Söll, unpublished result), which was kindly provided by D. Söll (Yale University, New Haven, CT), according to the protocol described by Hoben and Söll (1985). The protein was pooled and dialyzed against 20 mM K_2HPO_4 pH 7.2, 50 mM KCl, 1 mM DTT, and 50% glycerol for storage at −20 °C and 10 mM PIPES pH 7 and 1 mM DTT for crystallization (Perona, 1990). Aminoacylation assays were performed according to Hoben and Söll (1985).

Preparation of tRNA^{Gln} by Transcription in Vitro. Plasmids pUS618-CQ1 and pUS618-CQ2 (A. B. DiRenzo and O. C. Uhlenbeck, personal communication) in strain JM83 (Yanisch-Perron *et al.*, 1985) were a gift from O. C. Uhlenbeck (University of Colorado, Boulder, CO). The plasmids were derivatives of pUC18 with SP6 and T7 RNA polymerase-specific promoters followed by synthetic tRNA^{Gln} genes cloned into the polylinker site. In these two constructs, the U-A base pairs at position 1–72 of wild-type $tRNA_2^{Gln}$ were changed to a G-C in CQ1 and a G·A in CQ2 (A. B. DiRenzo and O. C. Uhlenbeck, personal communication). These changes were made, in part, because a G is required at position 1 for transcription by T7 RNA polymerase (Milligan *et al.*, 1987). Large-scale transcription *in vitro* with T7 RNA polymerase (a gift from D. Jeruzalmi, Yale University, New Haven, CT) from pUS618-CQ1 and pUS618-CQ2 digested with *Bst*NI (New England Biolabs) was performed according to the procedure described by Milligan *et al.* (1987) and modified to optimize the yield of these tRNAs. Reactions were carried out overnight (8 h) at 37 °C in 40 mM Tris-HCl pH 7.6, 24 mM $MgCl_2$, 2 mM spermidine, 10 mM dithiothreitol, 0.01% Triton X-100, and 100 mM KCl. The ratio of nucleoside triphosphates in the reaction was adjusted to correspond to the ratio of nucleotides in the RNA (Vioque *et al.*, 1988): 2.5 mM ATP, 3.3 mM GTP, 3.3 mM CTP, 2.5 mM UTP. T7 RNA polymerase (800 units/mL) was used to transcribe 160 μg of *Bst*NI-digested pUS618-CQ1 or pUS618-CQ2 per 1 mL of reaction for $tRNA_{G1\text{-}C72}^{Gln}$ or $tRNA_{G1}^{Gln}$, respectively. Adding polyethylene glycol (PEG) increased the generation of abortive transcripts while it did not affect the yield of tRNA.

After incubation of the transcription reaction for 8 h, the DNA was digested by addition of 5 μg of RNase-free DNase I (Worthington Biochemical Corp.) per milliliter of reaction and incubated for 2 h at 37 °C. EDTA was added to a final concentration of 50 mM to dissolve the precipitate (probably $Mg_2HP_2O_7$) generated during transcription. Then the transcripts were extracted once with one volume of phenol–chloroform 1:1 and twice with one volume of chloroform, precipitated with ethanol, and dried. They were resuspended in distilled water, loaded on a Sephadex G-25 (Pharmacia LKB Biotechnology Inc.) column (2.5-cm diameter × 16 cm), and eluted with water. Fractions containing the RNA were pooled, dried, resuspended in 40 mM Tris pH 7.6 and 24 mM $MgCl_2$, and reincubated with 10 μg/mL of DNase I for 3 h at 37 °C, and the steps from phenol–chloroform extraction to gel filtration were repeated. Sephadex G-25 fractions containing the tRNA transcript were pooled, aliquoted into several tubes, lyophilized, and stored at −20 °C until further use. The yield was 10–15 mg of tRNA transcript per 2 mg of digested plasmid DNA, which corresponded to a 230-fold amplification from the template. Just before crystallization trials an aliquot was dissolved in a small volume of distilled water.

Melting Temperature Determination. In order to compare structural stability of modified and unmodified tRNA^{Gln}, melting temperatures of $tRNA_{G1}^{Gln}$ and $tRNA_{G1\text{-}C72}^{Gln}$, both produced *in vitro*, and $tRNA_2^{Gln}$, produced *in vivo*, were determined as follows. PIPES pH 7.5 and $(NH_4)_2SO_4$ were added to the tRNAs dissolved in distilled water to the final concentrations of 50 and 30 mM, respectively. The changes in absorbance with increasing temperature were measured using a Perkin-Elmer UV–visible spectrometer #11250B Series PECSS Lambda 4B coupled to a Perkin-Elmer temperature programmer C570-0710 digital controller. The temperature was increased from 25 to 85 °C at a rate of approximately 1 °C/min. Four data sets were collected per tRNA variant. The data were processed and melting temperatures calculated as described by Cheong (1989) and Puglisi and Tinoco (1989). The melting temperatures were determined without the use of baselines, as they were found to be essentially the same as the values obtained in a case study with baselines.

Cocrystallization of tRNA^{Gln} Made in Vitro with GlnRS. GlnRS was complexed with $tRNA_{G1}^{Gln}$ or $tRNA_{G1\text{-}C72}^{Gln}$ prepared *in vitro* in a ratio of 2–8 mol of tRNA per 1 mol of GlnRS such that the final concentration of the complex was 10–15 mg/mL. Crystallization trials were set up at 17 °C using the hanging drop vapor diffusion method and conditions similar to those described by Rould *et al.* (1989) and Perona *et al.* (1988): 80 mM PIPES pH 6.5–7.5 or Tris-HCl pH 8,

Table 1: Summary of Collection and Reduction of X-ray Diffraction Data from Crystals of $tRNA^{Gln}$ Made *in Vitro* Complexed with GlnRS and ATP

resolution range	$R_{Friedel}$		no. of F_{obs}		percent complete	
	shell	cumul	expected	observed	shell	cumul
6.3–4.2	2.3	2.3	4035	2495	61.8	61.8
4.2–3.6	4.2	2.9	5189	4375	84.3	74.5
3.6–3.2	7.2	3.7	6144	4933	80.3	76.8
3.2–2.9	10.9	4.4	6947	5337	76.8	76.8
2.9–2.7	13.6	5.0	7681	5594	72.8	75.8
2.7–2.5	15.6	5.5	18 908	9934	52.5	66.8
6.3–2.5	5.5	5.5	48 904	32 668	66.8	66.8

20 mM $MgSO_4$, 0.02% NaN_3, 1.6–2.0 M $(NH_4)_2SO_4$, and 8 mM ATP.

Structure Determination. X-ray diffraction intensities from crystals of GlnRS complexed with ATP and $tRNA^{Gln}_{G1}$ produced by transcription *in vitro* were measured at −10 °C on a Xuong–Hamlin multiwire area detector using the University of California at San Diego data collection and reduction software (Howard *et al.*, 1985). Crystals had been stabilized in 2.3 M $(NH_4)_2SO_4$, 30 mM $MgSO_4$, 80 mM Na-PIPES pH 7.0, 0.02% NaN_3, 4 mM ATP, and 15% glycerol (Rould, 1991). Data were collected in the resolution range 7.5–2.4 Å. Three crystals were used to obtain a data set that was 67% complete between 6.3- and 2.5-Å resolution (Table 1). $R_{Friedel}$[3] was 5.5%, and the cross$R$[4] between this data set and a native data set of GlnRS complexed with $tRNA^{Gln}_2$ made *in vivo* was 13.8%. Data contained 67 255 observations of 33 367 reflections. The observed data were locally scaled to a native GlnRS – $tRNA^{Gln}_2$ATP data set using a procedure developed by Rould (1991, SCALAR); at least 200 reflections were used in each local scaling neighborhood.

A difference electron density map was calculated with the program X-PLOR (Brünger, 1990) using F_{obs}(GlnRS – $tRNA^{Gln}_{G1}$(made *in vitro*)–ATP) – F_{obs}(GlnRS – $tRNA^{Gln}_2$-(made *in vivo*)–ATP) as amplitudes, calculated phases derived from the refined structure model of the native complex at −10 °C (Rould *et al.*, 1991; Rould, 1991). The model used in the calculation of the phases had been refined with X-PLOR at 2.5-Å resolution, with the final crystallographic R-factor of 21%, root-mean-square (r.m.s.) bond deviations from ideality of 0.008 Å for the protein and 0.009 Å for the tRNA, and r.m.s. angle deviations from ideality of 2.3° for the protein and 3.2° for the tRNA (Rould *et al.*, 1991). The Brookhaven Protein Data Bank access code for the coordinates used is IGTS.

Model Building. Two water molecules were fitted to the difference Fourier electron density map and were hydrogen bonded to the pseudo-uridines in the anticodon region of $tRNA^{Gln}_2$. In other cases, *i.e.* at Ψ55 of $tRNA^{Gln}_2$ and the Ψ residues in the crystal structures of free $tRNA^{Phe}$ (Kim *et al.*, 1974; Suddath *et al.*, 1974) and $tRNA^{Asp}$ (Moras *et al.*, 1980; Westhof *et al.*, 1985), both from yeast, water molecules were modeled according to stereochemical principles. In all cases, water molecules with hydrogens were generated with X-PLOR (Brünger, 1990) and then manipulated with FRODO (Jones, 1982).

RESULTS

Thermal Stability of $tRNA^{Gln}$ Variants. The melting temperatures of $tRNA^{Gln}_2$, $tRNA^{Gln}_{G1\text{-}C72}$, and $tRNA^{Gln}_{G1}$ were determined to be 66, 65, and 62 °C (66.4 ± 0.5, 64.6 ± 0.7, and 62.2 ± 0.5 °C), respectively, under the conditions used. Four measurements per tRNA were performed. The profiles are shown in Figure 2. Both unmodified transcripts exhibit similar melting behavior, in contrast with that of the tRNA made *in vivo*, as shown by their relative absorbance profiles (Figure 2a). The curve tracing the fraction of $tRNA^{Gln}_{G1\text{-}C72}$ denatured (Figure 2b), however, approaches that of $tRNA^{Gln}_2$ near the midpoint, while that of $tRNA^{Gln}_{G1}$ is shifted entirely to the left. Thus, the melting temperature of the *in vitro* transcript with a mismatch at position 1–72 is about 4 °C lower than that of $tRNA^{Gln}_2$ produced *in vivo*, which is in good agreement with the results of Sampson and Uhlenbeck (1988). However, the transcript with the stronger G-C base pair at position 1–72 has nearly the same thermal stability as the modified variant.

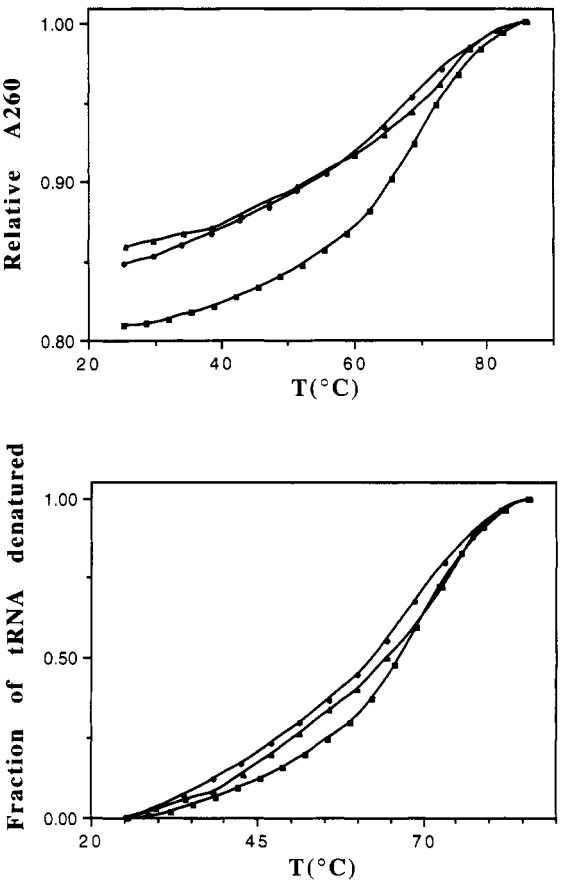

FIGURE 2: Melting profiles of (filled squares) $tRNA^{Gln}_2$ purified from overexpressing *E. coli* cells and (filled triangles) $tRNA^{Gln}_{G1\text{-}C72}$ and (filled circles) $tRNA^{Gln}_{G1\text{-}A72}$, both prepared by transcription *in vitro* with T7 RNA polymerase. Melting profiles were obtained in 50 mM PIPES pH 7.5 and 30 mM $(NH_4)_2SO_4$. (a, top) Relative absorbance at 260 nm vs temperature; the raw profiles were normalized to the absorbance at 85 °C. (b, bottom) Fraction of tRNA melted as a function of temperature, where the absorbance measured at 85 °C corresponds to 1 and that measured at 25 °C to 0. Each profile shown represents an average of four measurements.

Cocrystallization of $tRNA^{Gln}$ Made in Vitro with GlnRS. The complex of GlnRS with $tRNA^{Gln}_{G1}$, which has a mismatch in what is normally a base pair at position 1–72, gave better crystals than the complex of GlnRS with $tRNA^{Gln}_{G1\text{-}C72}$, whose base pairing at position 1–72 is restored by a C at position 72. At least a 2-fold molar excess of $tRNA^{Gln}$ made *in vitro* to GlnRS was essential for cocrystallization, in contrast to the 1:1 molar ratio that works when *in vivo* made tRNA is used; only precipitate was obtained when an equimolar amount of

[3] $R_{Friedel} = \Sigma_{hkl}|I_{hkl} - I_{\bar{h}\bar{k}\bar{l}}|/\Sigma_{hkl}(I_{hkl} + I_{\bar{h}\bar{k}\bar{l}})$

[4] cross$R$ = $\Sigma_{hkl}|I_{GlnRS\text{–}tRNA_{G1}} - I_{GlnRS\text{–}tRNA_2}|/\Sigma_{hkl}(I_{GlnRS\text{–}tRNA_{G1}} + I_{GlnRS\text{–}tRNA_2})$

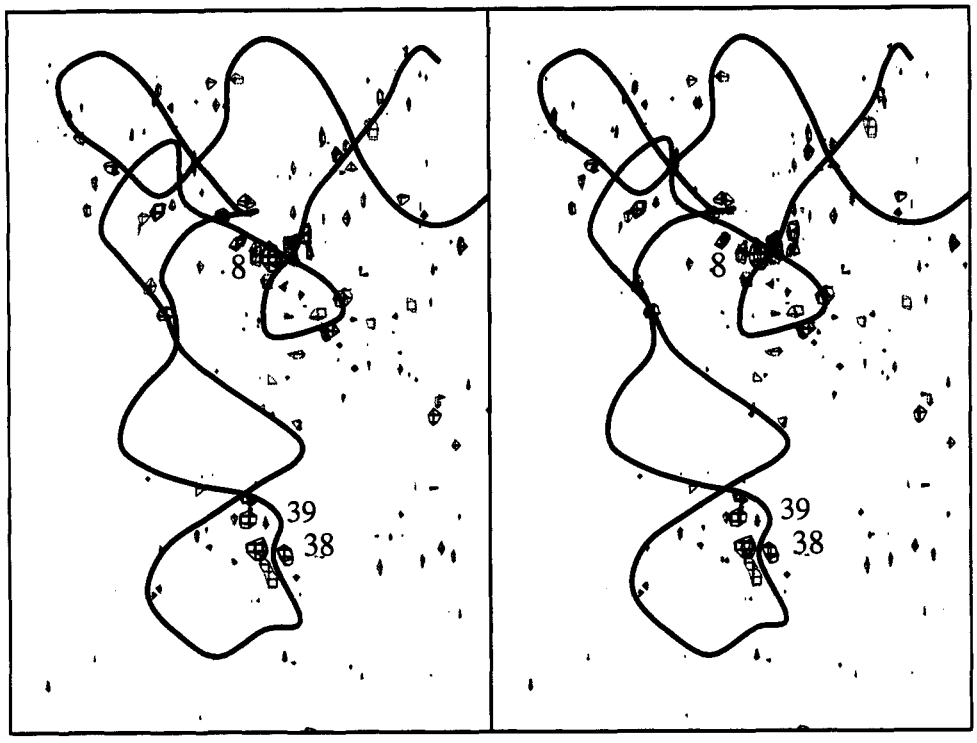

FIGURE 3: F_{obs}(GlnRS – $tRNA^{Gln}_{G1}$(made *in vitro*)) – F_{obs}(GlnRS – $tRNA^{Gln}_{2}$(made *in vivo*)) difference Fourier electron density map superposed on the model of $tRNA^{Gln}_{2}$ produced *in vivo* (Rould *et al.*, 1989; Rould *et al.*, 1991). In the model, the phosphates of the tRNA are traced in thick, solid black. In the map, positive differences are shown in light gray and negative differences in black. The map is contoured at 3.5σ, where 1σ = 1.8e/Å^3, and covers the entire molecule. This and subsequent figures were drawn using MINIMAGE (Arnez, 1994) followed by MOLSCRIPT (Kraulis, 1991).

$tRNA^{Gln}_{G1}$ or $tRNA^{Gln}_{G1\text{-}C72}$ to GlnRS was used in crystallization trials. The requirement for a large molar excess of tRNA might arise from conformational heterogeneity of the less stable unmodified tRNA, the length heterogeneity that occurs in tRNA transcripts, or both. Gel electrophoresis of the tRNA transcribed *in vitro* used in these cocrystallization experiments showed the presence of about 30% n + 1 and 30% n + 2 lengths in addition to the correct length. The difference map, however, shows no evidence of length heterogeneity at the highly ordered 3′ end of the tRNA.

Crystal Structure of $tRNA^{Gln}$ Made in Vitro Complexed with GlnRS. GlnRS complexed with $tRNA^{Gln}_{G1}$ (produced *in vitro*), and ATP crystallized isomorphously with the native complex made with $tRNA^{Gln}_{2}$ (made *in vivo*) (Rould *et al.*, 1989), in the space group $C222_1$, with unit cell dimensions a = 243.2, b = 94.2, and c = 116.2. An F_{obs}(GlnRS – $tRNA^{Gln}_{G1}$ – ATP) – F_{obs}(GlnRS – $tRNA^{Gln}_{2}$ – ATP) difference electron density map is shown in Figure 3, superposed on the model of the native complex.

The overall structure of GlnRS complexed with $tRNA^{Gln}_{G1}$ is identical to that of the native complex with $tRNA^{Gln}_{2}$. The differences seen in the difference Fourier map are minor and account mainly for the fact that the tRNA produced by transcription *in vitro* is unmodified. No difference in electron density is observed as a result of the uracil at position 1 being replaced by guanine; this is the anticipated result, since the native electron density map shows that the first base of $tRNA^{Gln}_{2}$ is disordered (Rould *et al.*, 1989; Perona, 1990; Rould, 1991). However, significant changes in electron density occur in the region of the Ψ38 and Ψ39 in the anticodon loop and a 4-thioU8.

The 4-thioU (4-sU) 8 of native $tRNA^{Gln}_{2}$ (Yaniv & Folk, 1975) is a U in $tRNA^{Gln}_{G1}$. The change of the sulfur at position 4 to an oxygen in the GlnRS – $tRNA^{Gln}_{G1}$ complex results in a reduction by 8 electrons and appears in the difference map (Figure 4) as a substantial loss of electron density at the nonring atom 4, an additional very small shift in the positions of the base of residue 8 and adjacent atoms in the tRNA that are seen in the difference Fourier map. Refinment of the coordinates of the complex with tRNA made *in vitro* was not done, since the differences in the structures of the two complexes implied by the difference map are smaller than the expected coordinate error at 2.5-Å resolution.

The anticodon loop of $tRNA^{Gln}_{2}$ contains the following modifications: 2-methyladenine of residue 37 and pseudouracils (Ψ) of residues 38 and 39 (Yaniv & Folk, 1975). The absence of the latter two modifications in $tRNA^{Gln}_{G1}$ is manifested by the loss of ordered water molecules which participate in a hydrogen bond network linking the N-5 of each Ψ to the backbone of $tRNA^{Gln}_{2}$. In addition, there is a slight shift in the phosphate of residue 37. This area is shown in detail in Figure 5a.

Native $tRNA^{Gln}_{2}$ also possesess three methylated nucleotides. However, methylations could not be discerned in this difference electron density map. One should be able to observe difference electron density that accounts for methyl groups, since differences accounting for water molecules are clearly indicated and since a methyl group possesses nearly as many electrons as a water molecule (9 and 10, respectively). The electron density differences corresponding to water molecules occur at a contour level greater than 5 standard deviations (σ, where 1σ = 1.8e/Å^3), and the differences between the sulfur and oxygen occur at a level greater than 7σ while the noise is below 3.5σ. Thus, the overexpressed native $tRNA^{Gln}_{2}$ cannot be fully methylated, though partial methylation would be undetected in these experiments.

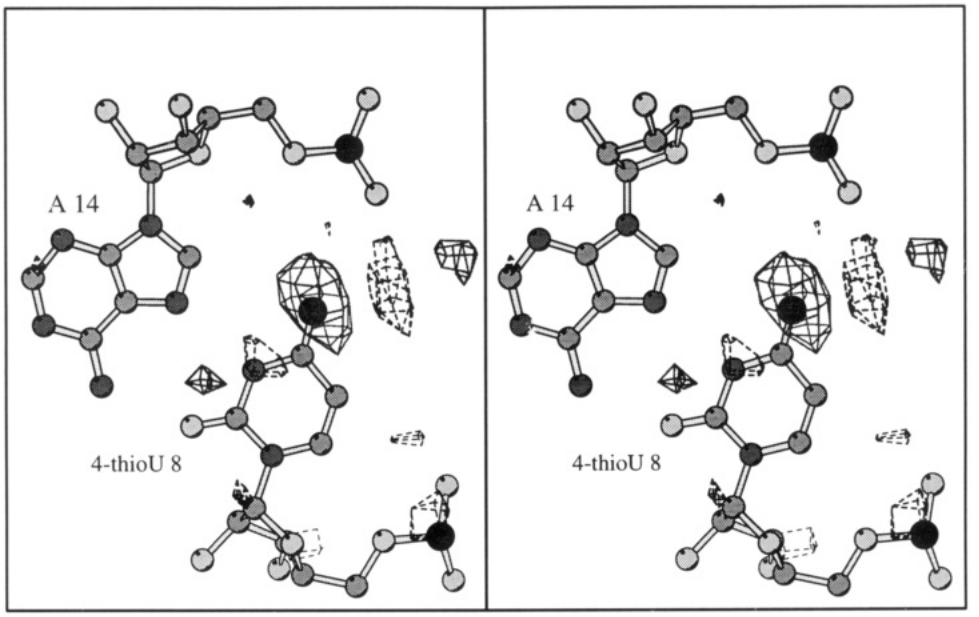

FIGURE 4: Detail of the map shown in Figure 3 showing the area at residue 8 viewed from the top. The positive differences in electron density are in dashed black, and the negative differences in solid gray lines.

The crystal structures of free $tRNA^{Phe}$ (Kim *et al.*, 1974; Suddath *et al.*, 1974) and $tRNA^{Asp}$ (Moras *et al.*, 1980; Westhof *et al.*, 1985) and that of $tRNA^{Gln}$ in complex with GlnRS (Rould *et al.*, 1989; Rould *et al.*, 1991) were examined for the presence of water molecules coordinated with the N-1 of a (Ψ) and the phosphodiester backbone in the manner of those at Ψ38 and Ψ39 in $tRNA_2^{Gln}$; none were found in the deposited coordinate sets. However, in all cases, including Ψ55 of $tRNA_2^{Gln}$, it was possible to introduce water molecules with similar hydrogen-bonding geometry by model building. A general coordination scheme is shown in Figure 5b, and individual model-building results are presented in Figure 6. Ψ13 of $tRNA^{Asp}$ does not follow exactly the general scheme, since the bridging water molecule would interact with the phosphate of residues 8 and 9 rather than 12 and 13, but the coordination geometry nevertheless appears to be similar.

DISCUSSION

This is the first crystal structure of an unmodified tRNA made *in vitro*, and it shows that $tRNA^{Gln}$ made *in vitro* complexed with GlnRS is structurally identical to $tRNA^{Gln}$ made *in vivo*. However, the observed differences in the water structure adjacent to the unmodified Ψ38 and Ψ39 suggest a role for the Ψ modification in stabilizing RNA structure.

In the crystal structure of GlnRS complexed with $tRNA_2^{Gln}$ (produced *in vivo*) and ATP, the terminal base pair of the tRNA is splayed out and the first residue is disordered in the electron density map (Rould *et al.*, 1989). Thus, Watson–Crick pairing of the two bases is not important *per se* and the substitution of a G for the U at position 1 of the *in vitro* transcript, which causes a mismatch, is more conservative than the substitution of the stronger G-C base pair for the original and weaker U-A. Biochemical experiments performed to test the transcripts and more detailed kinetics experiments (Jahn *et al.*, 1991) have shown that $tRNA_{G1}^{Gln}$ is a much better substrate for GlnRS than $tRNA_{G1\text{-}C72}^{Gln}$. The former is almost as good a glutamine acceptor as $tRNA_2^{Gln}$. Hence the ability of $tRNA_{G1}^{Gln}$ to form cocrystals with GlnRS that diffract to a higher resolution than crystals of $tRNA_{G1\text{-}C72}^{Gln}$ complexed with GlnRS is not surprising.

One of the factors that may make more than 2 mol of tRNA to 1 mol of GlnRS necessary to obtain cocrystals could be the lower thermal stability of *in vitro* transcripts. Increased flexibility has been demonstrated in several *in vitro* made tRNA systems through melting temperature shifts (Sampson & Uhlenbeck, 1988; Perret *et al.*, 1990b; Derrick & Horowitz, 1993) as well as increased accessibility to chemical agents and nucleases (Perret *et al.*, 1990b; Chow *et al.*, 1992; Derrick & Horowitz, 1993). When a tRNA binds to its cognate aminoacyl-tRNA synthetase, it undergoes a conformational change, as seen in the crystal structures of the complexes of GlnRS–$tRNA^{Gln}$ (Rould *et al.*, 1989; Rould *et al.*, 1991) and AspRS–$tRNA^{Asp}$ (Ruff *et al.*, 1991). Chemical and enzymatic accessibility patterns change as well, reflecting the same conformational changes in solution (Beresten *et al.*, 1992; Romby *et al.*, 1985). These patterns are slightly different when the tRNA is unmodified (Beresten *et al.*, 1992; Perret *et al.*, 1990b) and indicate higher accessibility of the uncomplexed, *in vitro* made tRNA. At the same time, NMR analyses (Hall *et al.*, 1989; Chu & Horowitz, 1989) as well as the present crystal structure suggest that the overall global structures of native fully modified tRNAs and their unmodified counterparts are the same. In the crystal structure the differences lie in the regions possessing modified nucleotides, whereas the rest of the structure is unchanged. This would indicate that the enzyme stabilied the tRNA, the crystal packing itself stabilized it, or both. Higher accessibility to probes in solution presumably indicates higher flexibility and "breathing" rate of the unmodified tRNAs as compared to their modified counterparts.

A comparison of the structures of $tRNA_2^{Gln}$ and $tRNA_{G1}^{Gln}$ complexed with GlnRS shows which residues are modified and the extent of modification in native $tRNA_2^{Gln}$ overproduced in *E. coli*. Three modifications that were deduced biochemically are observed in this structural analysis (Figure 1). Two features seen in the modified but not the unmodified $tRNA^{Gln}$ complexed with GlnRS are seen in this study: (1) the substitution of a sulfur atom for an oxygen at position 4 of uracil 8 and (2) two ordered water molecules

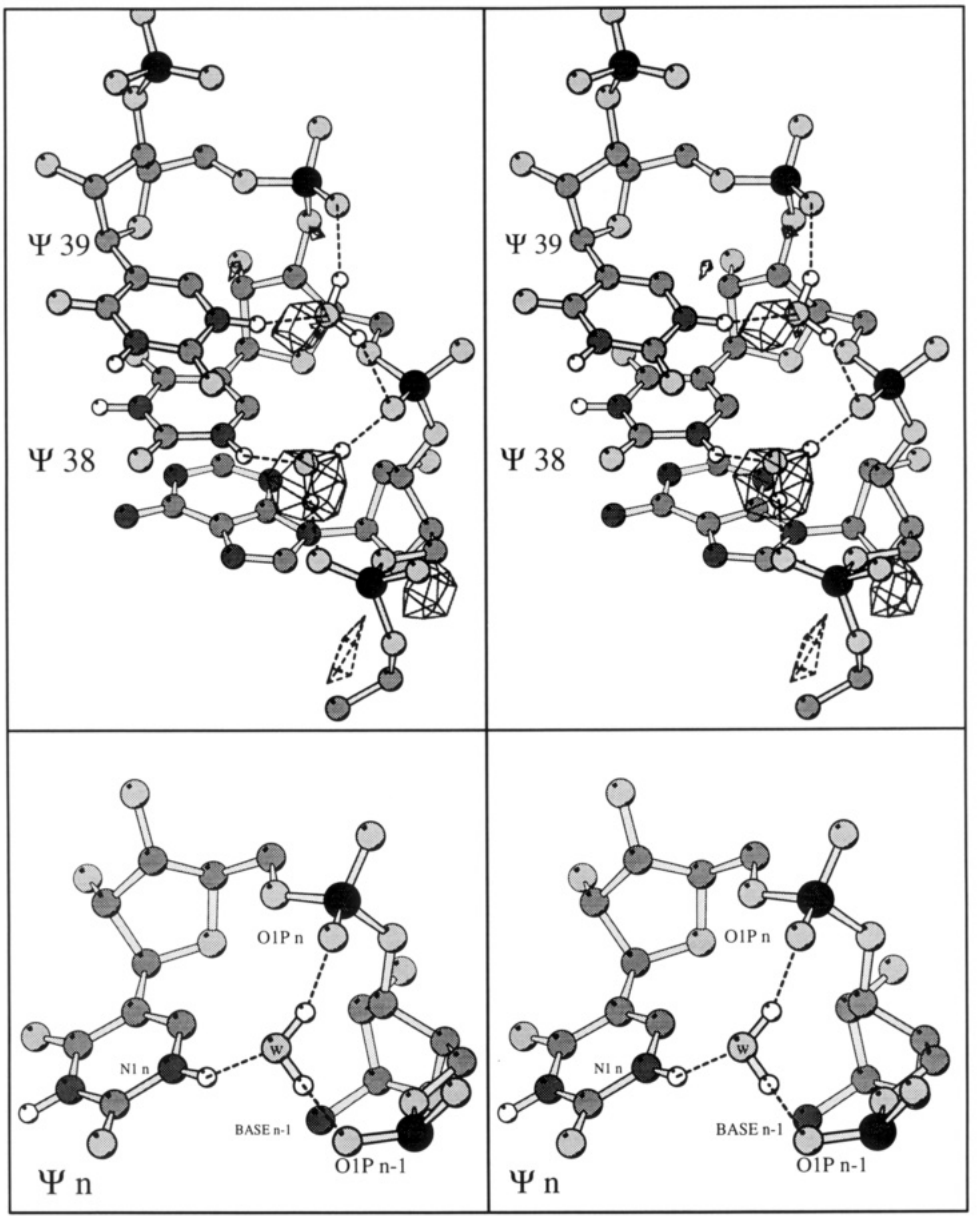

FIGURE 5: (a, top) Anticodon region of tRNA^{Gln}. A water molecule bridges the N-1 atom of each Ψ38 and Ψ39 and the phosphate oxygens of the backbone. Detail of the map shown in Figure 3 showing the disappearance of the two ordered water molecules when these two bases are not modified. The positive differences in electron density are in dashed black, and the negative differences in solid gray lines. (b, bottom) General hydrogen-bonding geometry of water molecules (W) at Ψ38 and Ψ39.

bridging the N-5 atoms of pseudo-uracils 38 and 39 and the phosphodiester backbone.

The role of the N-5 modification that exists in pseudo-uracil and not in uracil appears to be the stabilization of a particular RNA backbone structure resulting from a water-mediated cross-linking. In the case of both Ψ38 and Ψ39 the difference electron density map between the complex with modified and unmodified tRNA^{Gln} provides evidence that a water molecule is hydrogen bonded to the N-5 of the base as well as the 5′ phosphates of the nucleotide and the previous nucleotide (Figure 5). In contrast, there was no difference electron density corresponding to a water molecule adjacent to position 5 of Ψ55 in the TΨC arm. It is possible either that Ψ55 is undermodified in the tRNA^{Gln} overexpressed in *E. coli* or that water does not bind to the N-5 of Ψ55. However, the structural relationship between pseudo-uracil 55 and the phosphate backbone is identical to that of Ψ38 and Ψ39. A model-built water molecule inserted into the bridging position between the backbone and the base can make the same hydrogen bonds as observed at Ψ38 and Ψ39 (Figure 6).

Examination of the other known tRNA crystal structures suggests that this water-mediated cross-linking of pseudo-uracil to the phosphate backbone may be a common feature of pseudo-uracil and may identify a role for this modification in stabilizing a particular local RNA conformation (Figure 6). In addition to the case of Ψ55, which can form the water-bridged structure (Figure 6a) and presumably occurs as a common structural feature of all tRNA molecules, this water-mediated link between pseudo-uracil and the backbone is possible in Ψ13 and Ψ32 of tRNA^{Asp} (Moras *et al.*, 1980; Westhof *et al.*, 1985) (Figure 6b,c) and Ψ39 of tRNA^{Phe} (Kim *et al.*, 1974; Suddath *et al.*, 1974) (Figure 6d).

To assess what, if any, role the pseudo-uracil modification has in tRNA stability would require comparison of tRNA containing pseudo-uracils with unmodified tRNA of the identical sequence. However, due to the transcription initiation requirements of T7 RNA polymerase, the unmodified tRNA^{Gln} sequences available have either a G1-C72 base pair or a G1·A72 mismatch rather than the U1-A72 base pair found in the wild-type modified tRNA. Nevertheless, the melting

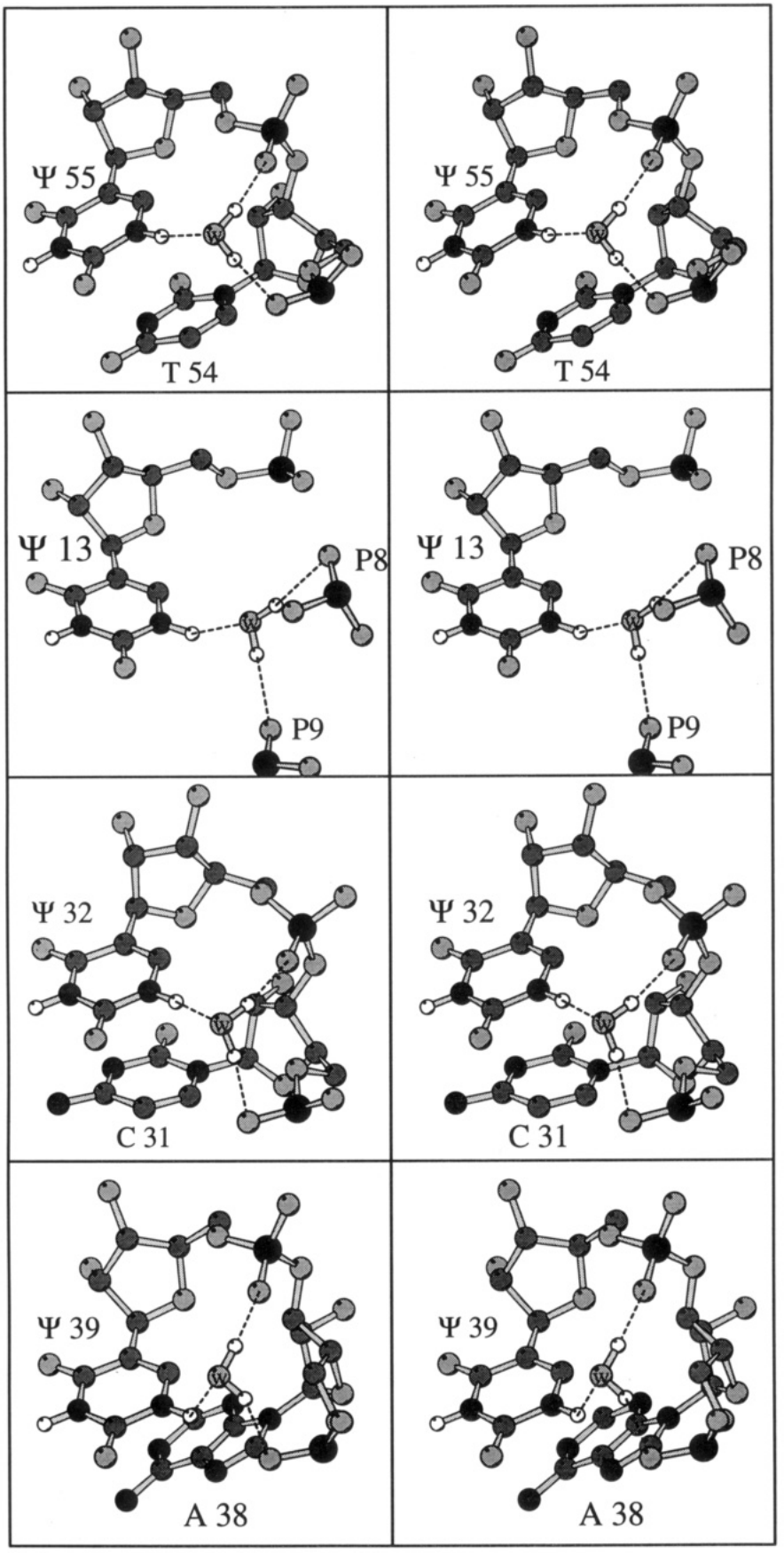

FIGURE 6: Pseudo-uridine residues of three tRNAs with modeled water molecules: (a, top) Ψ55 of $tRNA_2^{Gln}$ (Ψ55 of $tRNA^{Asp}$ and $tRNA^{Phe}$ are similar and are not shown); (b, second from top) Ψ13 of $tRNA_2^{Asp}$; (c, third from top) Ψ31 of $tRNA^{Asp}$; and (d, bottom) Ψ39 of $tRNA^{Phe}$.

temperature (T_m) data are consistent with the conclusion that the pseudo-uracil modifications do not stabilize the tRNA structure by more than the 4 °C that separates the *in vivo* made wild-type and *in vitro* made G1-A72 tRNAs but do stabilize it by more than the 1 °C difference between modified wild-type and unmodified G1-C72. What is unknown at

present is whether the unmodified tRNA has the same structure at Ψ38 and Ψ39 when not bound to GlnRS. If, indeed, interaction of the unmodified tRNA with the synthetase is required to form the observed tRNA structure at Ψ38 and Ψ39, then the affinity for unmodified tRNA would be somewhat less.

$tRNA_2^{Gln}$ that was overproduced in and purified from *E. coli* is probably undermethylated, since no difference in the methylation of residues, 17, 32, 37, and 54 between the *in vivo* and *in vitro* made tRNAs was observed in the difference Fourier map. Since the two water molecules at Ψ38 and Ψ39 were observed, and water molecules contain approximately as many electrons as methyl groups, the latter would have been observed had they been there. Undermethylation of $tRNA_2^{Gln}$ thus produced has been suggested before (Perona *et al.*, 1988). Apparently the methylases are not capable of keeping up with the overproduction of $tRNA_2^{Gln}$ in the cell. However, pseudouridinylation of certain uridines is a very efficient process (Samuelsson *et al.*, 1988). Melting profiles for fully modified $tRNA^{Gln}$ would most likely be different from those obtained with the undermodifiied $tRNA^{Gln}$ produced from overexpressing *E. coli*, and the melting temperature would be expected to be higher.

The fact that in complex with GlnRS wild-type $tRNA^{Gln}$ made *in vitro* is structurally identical to $tRNA^{Gln}$ made *in vivo* and the ability to cocrystallize a wild-type variant of $tRNA^{Gln}$ transcribed *in vitro* with GlnRS and ATP make crystallographic analyses of mutant variants of $tRNA^{Gln}$ made by transcription *in vitro* possible. The structure of wild-type $tRNA^{Gln}$ made *in vitro* complexed with GlnRS and ATP represents a control for structures of GlnRS complexed with variant tRNAs made by transcription *in vitro*, yet to be determined. Structures of complexes of GlnRS with mutant $tRNA^{Gln}$s made *in vitro* will show structural changes due to the mutations in $tRNA^{Gln}$.

ACKNOWLEDGMENT

J.G.A. is grateful to Dr. M. Rould for guidance with X-ray data processing and to Dr. S. Schultz for many useful discussions. We thank Prof. O. Uhlenbeck of the University of Colorado for supplying the two tRNA clones for transcription *in vitro*, D. Jeruzalmi for T7 RNA polymerase, and Prof. D. Söll for the *E. coli* strain overexpressing GlnRS.

REFERENCES

Arnez, J. G. (1994) *J. Appl. Cryst.*, in press.
Beresten, S.; Jahn, M., & Söll, D. (1992) *Nucleic Acids Res. 20*, 1523–1530.
Björk, G. R., Ericson, J. U., Gustafsson, C. E. D., Hagervall, C. E. D., Jönsson, Y. H., & Wikström, M. (1987) *Annu. Rev. Biochem. 56*, 263–287.
Brünger, A. T. (1990) *X-PLOR*, Yale Univesity, New Haven, CT.
Cheong, C. (1989) Ph.D. Thesis, University of California at Berkeley, CA.
Chow, C. S., Behlen, L. S., Uhlenbeck, O. C., & Barton, J. K. (1992) *Biochemistry 31*, 972–982.
Chu, W. C., & Horowitz, J. (1989) *Nucleic Acids Res. 17*, 7241–7252.
Derrick, W. B., & Horowitz, J. (1993) *Nucleic Acids Res. 21*, 4948–4953.
Hall, K. B., Sampson, J. R., Uhlenbeck, O. C., & Redfield, A. G. (1989) *Biochemistry 28*, 5794–5801.
Hoben, P., & Söll, D. (1985) *Methods Enzymol. 113*, 55–59.
Howard, A. J., Nielsen, C., & Xuong, Ng. H. (1985) *Meth. Enzymol. 114*, 452–472.
Jahn, M., Rogers, M. J., & Söll, D. (1991) *Nature 352*, 258–260.
Jones, T. A. (1982) in *Computational Crystallography* (Sayre, D., Ed.) p 303, Clarendon Press, Oxford, U.K.
Kim, S. H., Suddath, F. L., Quigley, G. J., McPherson, A., Sussman, J. L., Wang, A. H. J., Seeman, N. C., & Rich, A. (1974) *Science 185*, 435–440.
Kraulis, P. J. (1991) *J. Appl. Crystallogr. 24*, 946–950.
Milligan, J. F., Groebe, D. R., Witherell, G. W., & Uhlenbeck, O. C. (1987) *Nucleic Acids Res. 15*, 8783–8798.
Moras, D., Comarmond, M. B., Fischer, J., Weiss, R., Thierry, J. C., Ebel, J. P., & Giegé, R. (1980) *Nature 288*, 669–674.
Perona, J. J. (1990) Ph.D. Thesis, Yale University, New Haven, CT.
Perona, J. J., Swanson, R., Steitz, T. A., & Söll, D. (1988) *J. Mol. Biol. 202*, 121–126.
Perret, V., Garcia, A., Grosjean, H., Ebel, J. P., Florentz, C., & Giegé, R. (1990a) *Nature 344*, 787–789.
Perret, V., Garcia, A., Puglisi, J., Grosjean, H., Ebel, J. P., Florentz, C., & Giegé, R. (1990b) *Biochimie 72*, 735–744.
Puglisi, J. D., & Tinoco, I., Jr. (1989) *Methods Enzymol. 180*, 304–325.
Romby, P., Moras, D., Bergdoll, M., Dumas, P., Vlassov, V. V., Westhof, E., Ebel, J. P., & Giegé, R. (1985) *J. Mol. Biol. 184*, 455–471.
Rould, M. A. (1991) Ph.D. Thesis, Yale University, New Haven, CT.
Rould, M. A., Perona, J. J., Söll, D., & Steitz, T. A. (1989) *Science 246*, 1135–1142.
Rould, M. A., Perona, J. J., & Steitz, T. A. (1991) *Nature 352*, 213–218.
Ruff, M., Krishnaswamy, S., Boeglin, M., Poterszman, A., Mitschler, A., Podjarny, A., Rees, B., Thierry, J. C., & Moras, D. (1991) *Science 252*, 1682–1689.
Sampson, J. R., & Uhlenbeck, O. C. (1988) *Proc. Natl. Acad. Sci. U.S.A. 85*, 1033–1037.
Samuelsson, T., Borén, T., Johansen, T.-I., & Lustig, F. (1988) *J. Biol. Chem. 263*, 13692–13699.
Suddath, F. L., Quigley, G. J., McPherson, A., Sneden, D., Kim, J. J., Kim, S. H., & Rich, A. (1974) *Nature 248*, 20–24.
Vioque, A., Arnez, J., & Altman, S. (1988) *J. Mol. Biol. 202*, 835–848.
Westhof, E., Dumas, P., & Moras, D. (1985) *J. Mol. Biol.* bf 184, 119–145.
Yanisch-Perron, C., Vieira, J., & Messing, J. (1985) *Gene 33*, 103–119.
Yaniv, M., & Folk, W. R. (1975) *J. Biol. Chem. 250*, 3243–3253.